NASA TM X-125

TECHNICAL MEMORANDUM
X-125

APPROACH AND LANDING INVESTIGATION AT LIFT-DRAG RATIOS OF 3 TO 4 UTILIZING A DELTA-WING INTERCEPTOR AIRPLANE

By Gene J. Matranga and Joseph A. Menard

High-Speed Flight Station
Edwards, Calif.

NATIONAL AERONAUTICS AND SPACE ADMINISTRATION

WASHINGTON

October 1959

NATIONAL AERONAUTICS AND SPACE ADMINISTRATION

TECHNICAL MEMORANDUM X-125

APPROACH AND LANDING INVESTIGATION AT LIFT-DRAG RATIOS OF 3 TO 4 UTILIZING A DELTA-WING INTERCEPTOR AIRPLANE*

By Gene J. Matranga and Joseph A. Menard

SUMMARY

A series of landings was performed with a delta-wing interceptor airplane to evaluate the effect of low lift-drag ratios on approach and landing characteristics. Landings with peak effective lift-drag ratios as low as 3.75 were made by altering the airplane configuration (reducing the throttle setting to idle, and extending speed brakes, missile-bay doors, and gear).

The altitude, indicated airspeed, vertical velocity, and flight-path angle at the initiation of flare, and the time to flare increased noticeably with the reduction in lift-drag ratio. However, the pilots reported that all approaches and landings were comfortable, with ample time and control available for any required corrections.

A comparison of the data from these tests with the results of tests made on a straight-wing fighter airplane having twice the wing loading shows that the data are similar, but with several notable exceptions. The speeds for the delta-wing interceptor were markedly slower, the high key point (initial point) was considerably lower, the pattern was much tighter, and the flight-path angles at the initiation of flare were higher than for the straight-wing airplane which had a greater wing loading. Pilot comment indicated that the subject airplane was more comfortable than the straight-wing airplane in the approach pattern for the same lift-drag ratio, but that the airplanes exhibited similar characteristics during the flare.

When flying specific calculated landing patterns, the pilot reported difficulty in determining the initial point accurately without external guidance; however, he was successful in locating the initial point during these landings and indicated that the patterns were easy and comfortable to fly.

*Title, Unclassified.

INTRODUCTION

Among the many configurations under consideration for hypersonic and entry vehicles are delta-wing configurations with extreme sweep. Although such vehicles may furnish the optimum design for hypersonic flight or entry, many problems are introduced at low speed in the approach and landing pattern even though the vehicles are generally characterized by low wing loadings and the associated low forward velocities. Some of the more pronounced problem areas include the approach and landing patterns at low lift-drag ratios, which are characterized by steep flight-path angles, high flare altitudes, and objectionably high sink rates close to the ground. A limited landing investigation probing into some of these areas was performed with several research airplanes, including the delta-wing XF-92A research airplane. The results of this investigation were reported in reference 1. Subsequently, a more complete flight investigation of landings at low lift-drag ratios was conducted at the NASA High-Speed Flight Station, Edwards, Calif., using a delta-wing interceptor having a wing loading of 35 pounds per square foot. The results of this investigation are presented herein and are compared with the results reported in reference 2, which were obtained with a straight-wing fighter airplane having a similar lift-drag-ratio range but having twice the wing loading. Also included are the results obtained with the delta-wing interceptor when the pilot attempted to fly computed approach patterns based upon the use of constant airspeed and constant bank angle throughout the pattern.

SYMBOLS

All lift and drag quantities are referenced to the airplane flight path.

a_n normal acceleration, g units

$a_{n_{max}}$ maximum normal acceleration during flare, g units

C_D drag coefficient, $\frac{D}{qS}$

C_L lift coefficient, $\frac{L}{qS}$

D airplane drag, lb

D'	effective drag, D - (thrust)cos α, lb
D_e	equivalent airplane drag, $D' + \frac{W}{g}\dot{V}$, lb
F	centripetal force, lb
g	acceleration due to gravity, ft/sec^2
h	geometric altitude above touchdown point, ft
L	airplane lift, lb
L'	effective lift, L + (thrust)sin α, lb
L/D	lift-drag ratio
$(L/D)'$	effective lift-drag ratio, $\frac{L'}{D'}$
n'	load factor, $\frac{L'}{W}$
q	dynamic pressure, lb/sq ft
r	radius of ground path, ft
S	wing area, sq ft
t	time prior to touchdown, sec
V	true airspeed, ft/sec
$\dot{V}$	derivative of airspeed with time, $\frac{dV}{dt}$, ft/sec^2
V_i	indicated airspeed, knots
V_v	vertical velocity, ft/sec
W	airplane weight, lb
x	longitudinal distance from touchdown point, ft
y	lateral distance from touchdown point, ft
α	angle of attack, deg

Δt	time from initiation of flare to touchdown, sec
ΔV_i	increment in indicated airspeed during flare, knots
γ	flight-path angle, deg
φ	bank angle, deg

Subscript:

f	conditions at initiation of flare

INSTRUMENTATION

The following pertinent quantities were recorded on NASA internal-recording instruments which were synchronized by a common timer:

Airspeed and altitude

Normal and longitudinal accelerations

Pitching velocity and acceleration

Angle of attack

Control positions and control-surface positions

Airspeed, pressure altitude, and angle of attack were sensed on the nose boom; angle of attack was corrected for the effects of pitching velocity, pitching acceleration, and normal acceleration.

To ascertain more accurately the airplane location during the approach and landing, ground aids were utilized. A modified SCR 584 radar phototheodolite was used to measure the location of the airplane in space down to an altitude of about 1,000 feet. Below this altitude Air Force Flight Test Center Askania Cine-Theodolite cameras indicated the location of the airplane.

AIRPLANE

The test airplane is a single-place, delta-wing interceptor powered by a turbojet engine equipped with afterburner. A three-view drawing and a photograph of the airplane are shown in figures 1 and 2, respectively. The physical characteristics of the airplane are presented in table I.

The airplane is characterized by a nominal 4-percent-thick delta wing having an aspect ratio of 2.08. Speed brakes located at the base of the vertical tail near the trailing edge and missile-bay doors located on the undersurface of the fuselage were utilized to provide the additional drag which was employed to obtain the low lift-drag-ratio conditions reported in this paper.

The longitudinal and lateral controls employ dualized irreversible hydraulic systems, with bungees providing artificial feel. In addition to the bungee system a dynamic-pressure-sensing device in the longitudinal- and directional-control systems is used to vary the control forces with airspeed, and to compensate for the unstable longitudinal stick-force variations in the transonic region. Longitudinal and lateral control are provided by elevons located on the trailing edge of the wing, and directional control is provided by a conventional rudder.

No artificial damping was provided during any of the approach and landing maneuvers performed in this investigation.

TESTS

Fifteen landings were performed to evaluate the approach and landing characteristics at low lift-drag ratios. The average wing loading during these landings was about 35 pounds per square foot. Two pilots participated in this investigation. During most of these tests, the only instruction given the pilots prior to the landings was that a specified configuration and engine-power setting be maintained throughout any given approach and landing maneuver. The pilots were free to terminate the approach at any time and availed themselves of this prerogative on four occasions as a result of aircraft-traffic considerations. All landings were performed on the 15,000-foot east-west runway at Edwards Air Force Base, Calif. Because the pilot was not attempting to touch down at a specific point, no analysis of contact dispersion was made.

For the initial landings constant power settings near 80-percent engine rpm were utilized. As the pilot became familiar with the handling qualities of the low lift-drag-ratio configuration, landings were performed with successively lower constant power settings until the engine speed was reduced to idle.

Five landings were performed attempting to fly a computed pattern, inasmuch as it was believed that such a pattern might ease some of the pilot-judgment problems normally involved in landing at low lift-drag ratios. At the high key point (initiation of descent) the pilot established a constant, predetermined airspeed and bank angle and maintained

these conditions down to an altitude of about 1,000 feet, at which point he was in a position to perform his final flare.

A discussion of the data-reduction techniques utilized for the present investigation is presented in reference 2.

RESULTS AND DISCUSSION

The basic aerodynamic relationships of angle of attack, drag coefficient, and lift-drag ratio as a function of lift coefficient for the airplane at low lift-drag ratios (extended speed brakes, missile-bay doors, and gear) are shown in figure 3. These data, compiled from several landing approaches, show that the drag coefficient rises sharply from a value of 0.077 at a lift coefficient of 0.22 to a value of 0.17 at a lift coefficient of 0.52. Although the peak value of lift-drag ratio is slightly above 3.5, the peak value of effective lift-drag ratio, which includes the effects of engine thrust, is somewhat larger. The average 300 pounds of thrust at idle power settings increased the peak effective lift-drag ratio to a value of 3.75.

Landing Pattern

A typical approach and landing maneuver performed with the test airplane at low lift-drag ratios is illustrated in figure 4. Figure 4(a) presents the landing pattern, figure 4(b) presents the time history of the approach and landing, and figure 4(c) presents the time history of the flare. The pilot performed a 270° overhead approach with the high key point at an altitude of 12,500 feet above a point 7,000 feet down the runway from the touchdown point. Maximum longitudinal and lateral distances away from the touchdown point were 10,000 and 14,000 feet, respectively (fig. 4(a)). The forward speed was generally 200 knots indicated airspeed throughout the approach. The average rate of sink during the approach was about 100 feet per second, with a peak value of 140 fps (fig. 4(b)).

The pilots reported that the patterns flown were comfortable, with the maximum bank angle employed being slightly in excess of 30°. Hitting a desired touchdown point was found to be relatively simple; the airplane touched down approximately on the point at which the vehicle had been pointed during the final approach.

A comparison of the approach patterns flown with the test airplane and with the airplane of reference 2 shows several notable differences. For comparable lift-drag ratios the high key point for the subject airplane was about 10,000 feet lower and the pattern was considerably

tighter than for the straight-wing fighter airplane. Also, the approach speeds were generally 50 to 60 KIAS slower with the delta-wing airplane; consequently, the sink rates were about 60 fps lower. The prime reason for these differences is that the wing loading of the straight-wing fighter is more than double that of the delta-wing interceptor.

As was reported in reference 2, the 270° approach is preferred by the pilot because of the greater ease afforded in visually positioning the airplane. This general conclusion was also reached, independently, by a pilot of the NASA Langley Research Center and was reported in reference 3.

Flare

Just before the airplane was alined with the runway, the pilot initiated the flare (fig. 4(c)). This flare, defined in terms of flight-path deviation, was initiated about 16 seconds prior to touchdown and was performed from an initial altitude of 600 feet with an initial forward speed slightly greater than 190 KIAS. The initial vertical velocity was slightly less than 85 fps. The touchdown was accomplished with a forward velocity of 143 KIAS and a vertical velocity of less than 1 fps. The maximum normal acceleration used during the flare was 1.27g, and the maximum angle of attack was 14.6°.

Figure 5 summarizes the parameters which seem to illustrate best the flare characteristics during the low lift-drag-ratio landings. Initial vertical velocity, initial indicated airspeed, initial altitude, initial flight-path angle, maximum normal acceleration used during the flare, time required to flare, and change of airspeed during the flare are plotted as a function of effective lift-drag ratio at the initiation of flare. Shown in this figure, for comparison purposes, are similar data from a normal landing. As the effective lift-drag ratio at the initiation of flare was reduced from just above 4 to 3.4, the altitude at the initiation of flare increased rapidly from slightly above 300 feet to just under 1,000 feet, and the initial airspeed increased from about 180 KIAS to slightly over 200 KIAS. Correspondingly, the vertical velocity at the initiation of flare also increased from almost 60 fps to over 100 fps. As expected, the reduction in lift-drag ratio resulted in an increase in the initial flight-path angle from about 12.5° to 20°, and the time required to execute the flare increased from about 10 seconds to about 20 seconds. The change in airspeed during the flare increased slightly to a value of 50 KIAS with the reduction in lift-drag ratio. Only the values of maximum normal acceleration used during the flare remained relatively constant, with an average value of about 1.3g.

A comparison of these data with the summary flare data of reference 2 shows that all trends were similar for the two aircraft used in

these studies in the same $(L/D)'$ range. However, the airspeed at the initiation of flare for the subject airplane is about 50 KIAS lower, the change in airspeed during flare is about 30 KIAS less, and the maximum normal acceleration used is about 0.1g lower than the values reported in reference 2. The initial flight-path angle is, however, about 4° higher. This difference of 4° is attributable to the fact that the straight-wing fighter airplane performed an initial flare just below an altitude of 10,000 feet, and, consequently, the change of speed associated with this initial flare reduced the flight-path angle at the initiation of the final flare.

It is of interest to note that the rate of sink at touchdown was as high as 3 fps on only two occasions. These values are similar to those presented in reference 1 and only slightly higher than those reported in reference 2, but are well below the design value. In commenting on rates of sink at touchdown, the pilots reported ground effect was not as noticeable on the test airplane as it was on the straight-wing airplane of reference 2.

Pilot Comment

Pilot impressions and opinions provide additional information on the subject of landing in the region of low lift-drag ratios. One of the pilots participating in this investigation also took part in the tests reported in reference 2, and thus based many of his comments upon this previous experience. Up to the point of flare initiation, the pilots considered the pattern comfortable, with ample time and control available for any required corrections. This apparent ease, as compared with the reportedly severe approaches of reference 2 (even in the same lift-drag-ratio range), was due primarily to the slower speeds and expanded time scale of the subject landing study. The author-pilot of reference 3 also expressed the view that slower approach speeds were preferable because of the difference in judgment and control involved.

As in the investigation reported in reference 2, the pilots felt they could not set forth any specific criterion upon which they based their initiation of flare. Rather, they indicated that it depends upon the interrelationship of many factors, including speed, altitude, rate of sink, and position with respect to the desired touchdown point. Flare characteristics for this airplane were reported to be similar to those of the airplane of reference 2. However, the pilots preferred the delta-wing vehicle because of the greater lift margin available for flare. Only below a flare-initiation speed of 175 KIAS did the pilots believe difficulties might be expected because of the reduced speed margin and reduced lateral control available at the large elevon deflections used for longitudinal trim and control.

Ability to Fly Computed Patterns

To insure a safe landing of any vehicle having a low lift-drag ratio, such as an unpowered orbital vehicle, it would be advantageous to specify beforehand the pattern entry altitude, airspeed, and bank angle to be maintained throughout the approach. Accurate predicted patterns may be obtained by using a digital computer, but simplified calculations can provide patterns of reasonable accuracy. Patterns were manually calculated by the method detailed in the appendix and were subsequently flown with the test airplane to verify the predictions. These computed flight paths were based upon standard atmospheric conditions and zero-wind considerations. The winds actually experienced in flight reached values up to 20 knots, however. The pilot used no corrective action to compensate for these winds.

Prior to the flight the pilot was instructed to arrive at the high key point with a specific altitude, airspeed, and configuration, then fly a specified bank-angle turn and airspeed. The pattern was designed to terminate off the approach end of the runway at an altitude of 1,000 feet as the airplane completed the final turn onto the runway. The pilot would then flare at his own discretion.

A comparison of the computed pattern with the patterns actually flown during five approach and landing maneuvers is shown in figure 6. These patterns called for a high key point at 15,000 feet, a constant airspeed of 200 KIAS, and a bank angle of 30°. The flight patterns and computed patterns are in good agreement.

Since exact positioning is difficult to determine from altitudes near 15,000 feet, the pilot felt the most difficult part of the pattern was to locate accurately the high key point. Figure 6 shows he was successful in the five maneuvers performed. By making minor bank-angle corrections, the pilot experienced no difficulty in arriving at the flare point. He reported that the computed pattern was comfortable, easy to fly, and worthy of further study.

It is believed that the pilot's task could be eased somewhat if he were to be guided to the initial point by ground radar and if radar surveillance were maintained throughout the pattern.

CONCLUDING REMARKS

During a series of landings with a delta-wing interceptor airplane, peak effective lift-drag ratios as low as 3.75 were achieved by altering the airplane configuration (reducing throttle setting to idle, and extending speed brakes, missile-bay doors, and gear).

As the effective lift-drag ratio at the initiation of flare was reduced from slightly more than 4 to 3.4, the time to flare, altitude, indicated airspeed, vertical velocity, and flight-path angle at the initiation of flare increased noticeably even though the pilots reported that all approaches and landings were comfortable, with ample time and control available for any required corrections.

A comparison of data for the test airplane and a straight-wing fighter airplane having twice the wing loading shows that the data are similar, but with several notable exceptions. The speeds for the delta-wing airplane were markedly slower, the high key point was considerably lower, the pattern was much tighter, and the flight-path angles at the initiation of flare were higher than for the straight-wing airplane which had a greater wing loading. Pilot comment indicated that for the same lift-drag ratio the subject airplane was more comfortable than the straight-wing airplane in the approach pattern, but during the flare the airplanes exhibited similar characteristics.

When flying specific calculated landing patterns, the pilot reported difficulty in accurately determining the initial point without external guidance, even though data show that he was successful in locating the initial point during these landings. He further reported that the patterns were easy and comfortable to fly.

High-Speed Flight Station,
National Aeronautics and Space Administration,
Edwards, Calif., July 27, 1959.

APPENDIX

METHOD USED TO CALCULATE THE LANDING PATTERN

The airplane is in banked flight, as shown in the following sketch:

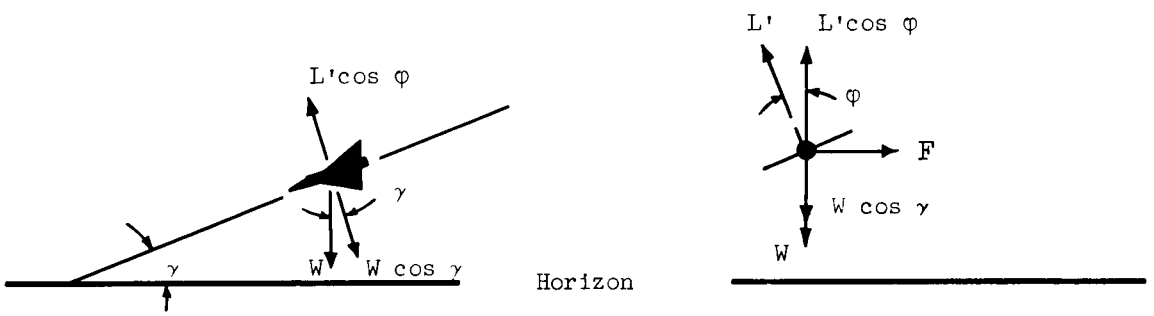

Equating the lift and weight vectors

$$W \cos \gamma = L' \cos \varphi \tag{1}$$

or, rearranging terms

$$\frac{L'}{W} = \frac{\cos \gamma}{\cos \varphi} \tag{2}$$

which is load factor n'. The flight-path angle γ may be approximately determined as

$$D' + \frac{W}{g} \dot{V} = W \sin \gamma \tag{3}$$

Let

$$D_e = D' + \frac{W}{g} \dot{V} \tag{4}$$

so that from equation (3)

$$\frac{D_e}{W} = \sin \gamma \tag{5}$$

$$\dot{V} = \frac{dV}{dh}\left(\frac{dh}{dt}\right) = (V \sin \gamma)\frac{dV}{dh} \tag{6}$$

Substituting for $\dot{V}$ in equation (4)

$$D_e = D' + \frac{W}{g}(V \sin \gamma)\frac{dV}{dh} \tag{7}$$

and substituting for $\sin \gamma$ in equation (7)

$$D_e = D' + \frac{WV}{g}\left(\frac{D_e}{W}\right)\frac{dV}{dh} = \frac{D}{1 - \frac{V}{g}\frac{dV}{dh}} \tag{8}$$

Then, dividing equation (8) by the effective lift L'

$$\frac{D_e}{L'} = \frac{D'/L'}{1 - \frac{V}{g}\frac{dV}{dh}} \tag{9}$$

Expanding equation (5) and relating it to equation (2)

$$\sin \gamma = \frac{D_e}{W} = \left(\frac{D_e}{L'}\right)\left(\frac{L'}{W}\right) = n' \frac{D_e}{L'} \tag{10}$$

If constant dynamic pressure and constant thrust are assumed during the descent, equation (9) may be solved in steps considering average values of D'/L', V, and dV/dh. Assuming a constant load-factor turn, the flight-path angle may then be found.

The landing pattern may be drawn by computing the radius of the ground path. Since the centripetal force created during a turn must be opposed by a portion of the lift

$$F = \frac{W}{g}\frac{(V \cos \gamma)^2}{r} = L' \cos \gamma \sin \Phi \qquad (11)$$

so that

$$r = \frac{W(V \cos \gamma)^2}{gL' \cos \gamma \sin \Phi} = \frac{V^2 \cos \gamma}{gn \sin \Phi} \qquad (12)$$

The pattern is assumed to be made up of circular segments, each having a different constant radius r as shown in the following sketch. The value of r should be recomputed at each 2,000-foot change of altitude during the descent.

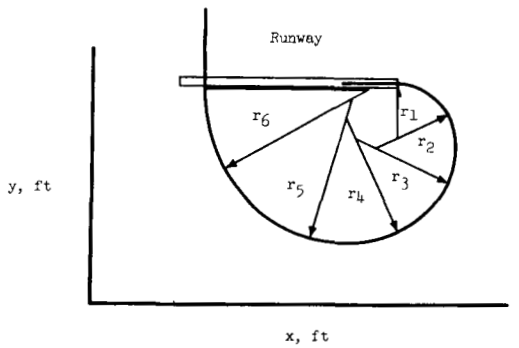

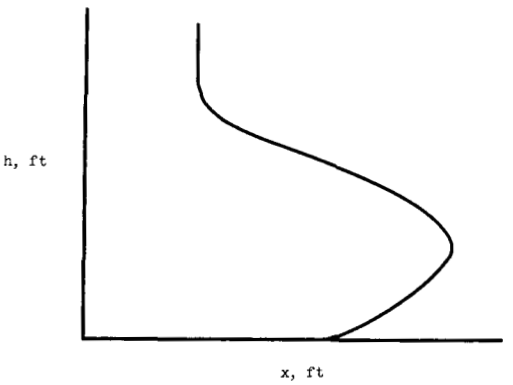

REFERENCES

1. Stillwell, Wendell H.: Results of Measurements Made During the Approach and Landing of Seven High-Speed Research Airplanes. NACA RM H54K24, 1955.

2. Matranga, Gene J., and Armstrong, Neil A.: Approach and Landing Investigation at Lift-Drag Ratios of 2 to 4 Utilizing a Straight-Wing Fighter Airplane. NASA TM X-31, 1959.

3. Reeder, John P.: The Effect of Lift-Drag Ratio and Speed on the Ability to Position a Gliding Aircraft for a Landing on a 5,000-Foot Runway. NASA MEMO 3-12-59L, 1959.

TABLE I.- TABLE OF PHYSICAL CHARACTERISTICS

Wing:	
Airfoil section	NACA 0004-65 (Modified)
Total area, sq ft	695.05
Span (actual), ft	38.17
Mean aerodynamic chord, ft	23.76
Root chord, ft	35.63
Tip chord, ft	0.81
Taper ratio	0.023
Aspect ratio	2.08
Sweep at leading edge, deg	60.1
Sweep at trailing edge, deg	-5
Incidence, deg	0
Dihedral, deg	0
Conical camber (leading edge), percent local semispan	6.3
Geometric twist, deg	0
Inboard fence, percent semispan	37
Outboard fence, percent semispan	67
Tip reflex, deg	6
Maximum thickness -	
Root, percent	3.9
Outboard edge of elevon, percent chord	3.5
Approximate test wing loading, lb/sq ft	35
Elevons:	
Area (total, rearward of hinge line), sq ft	67.2
Span (one elevon), ft	12.89
Vertical tail:	
Airfoil section	NACA 0004-65 (Modified)
Area (above waterline 33), sq ft	95.1
Aspect ratio	1.4
Sweepback of leading edge, deg	52.5
Sweepback of trailing edge, deg	0
Fuselage:	
Length, ft	63.3
Maximum diameter, ft	6.5
Total inlet capture area, sq ft	4.6
Equivalent-body fineness ratio	9.1
Speed brakes (per side):	
Area -	
Flat plate, sq ft	9.48
Projected frontal area at maximum deflection, sq ft	6.70
Chord, ft	4
Deflection limit, deg	45
Power plant:	
Installed static thrust at sea level, lb	8,800
Installed static thrust at sea level, (with afterburner), lb	13,200
Test center-of-gravity location, percent mean aerodynamic chord	28 to 29
Average landing weight, lb	24,000

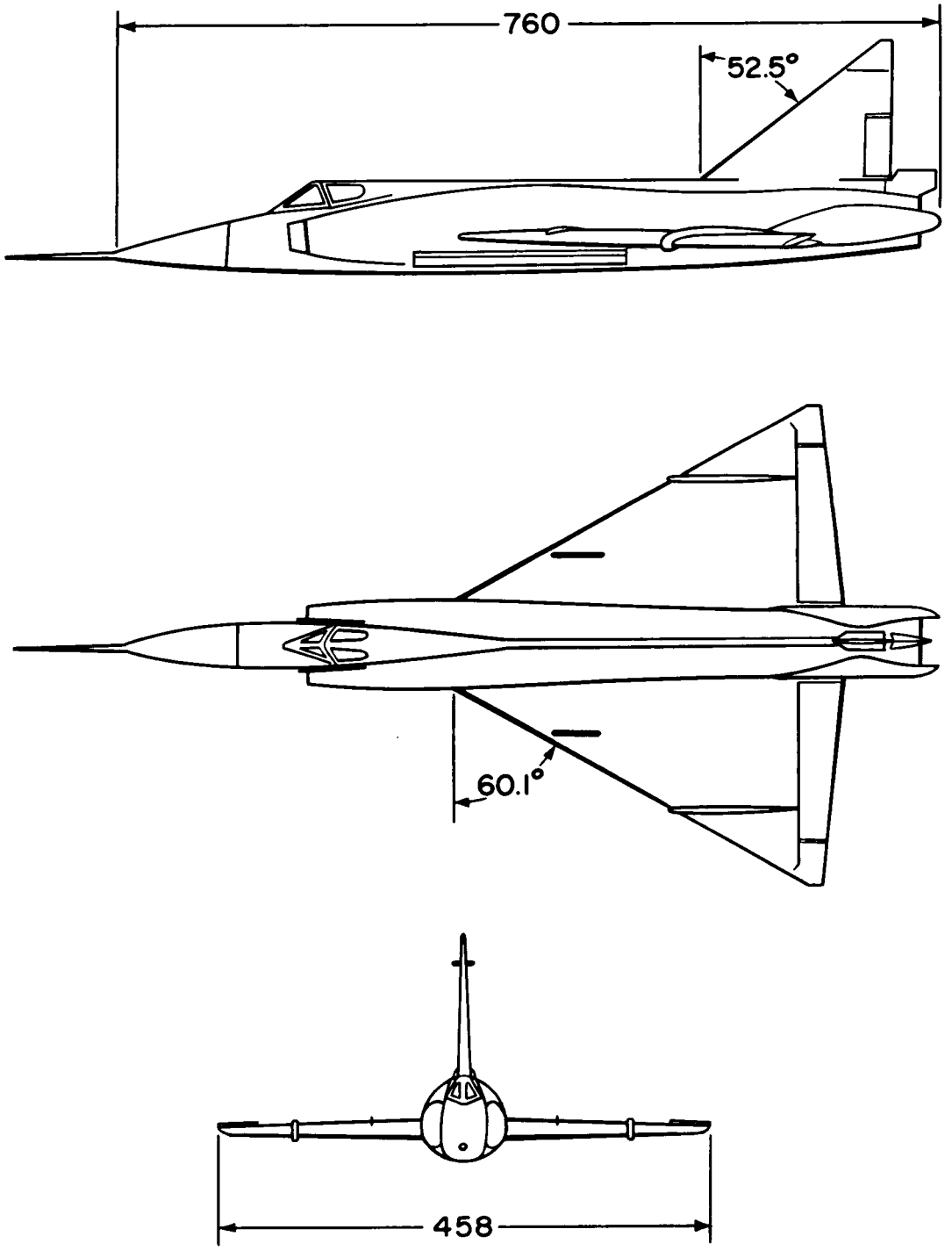

Figure 1.- Three-view drawing of the test airplane. All dimensions in inches.

E-4504

Figure 2.- Photograph of the test airplane with the gear and missile-bay door fully extended and the speed brake partially extended.

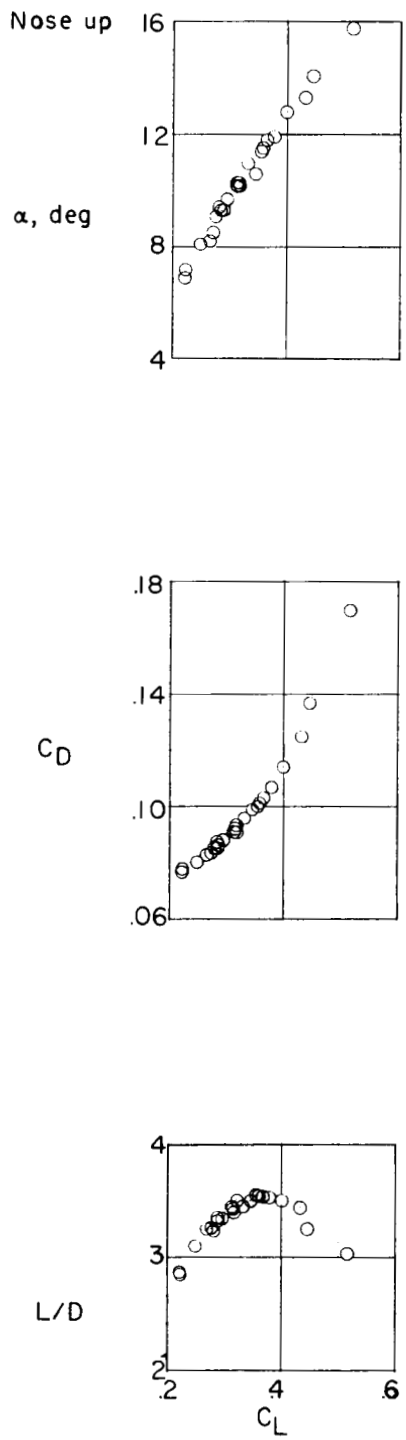

Figure 3.- Angle of attack, drag coefficient, and lift-drag ratio presented as a function of lift coefficient at low lift-drag ratios.

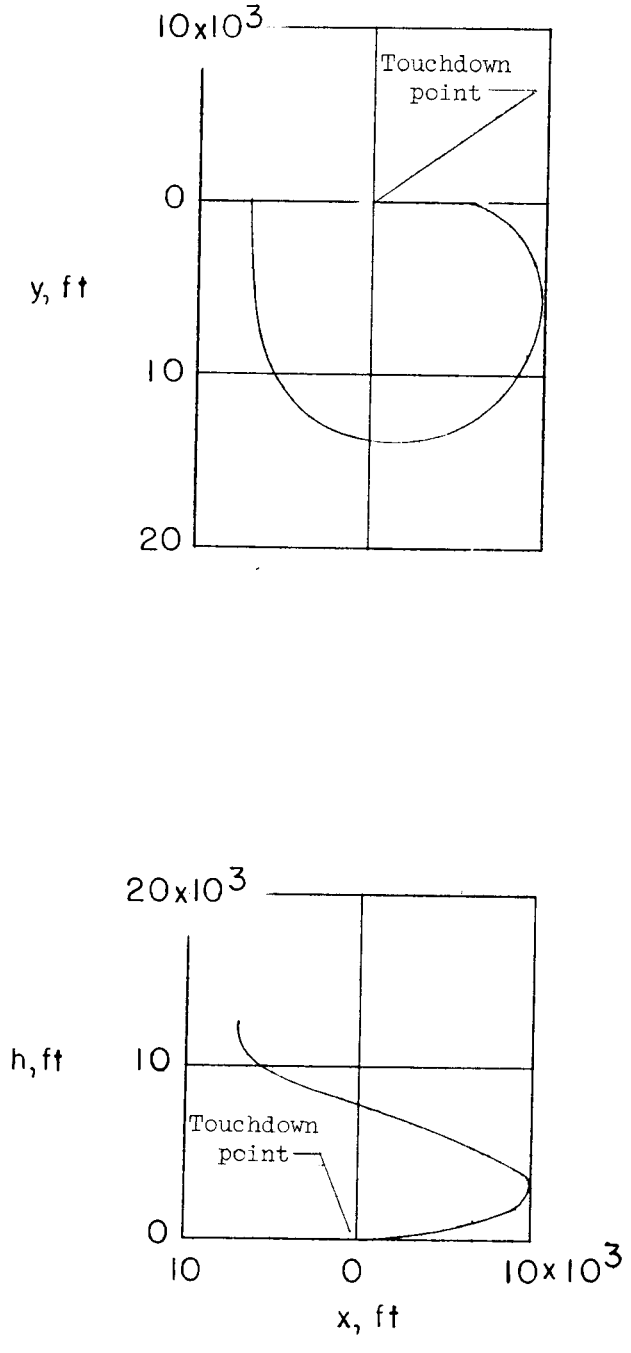

(a) Landing pattern.

Figure 4.- Typical approach and landing characteristics for the test airplane at low lift-drag ratios.

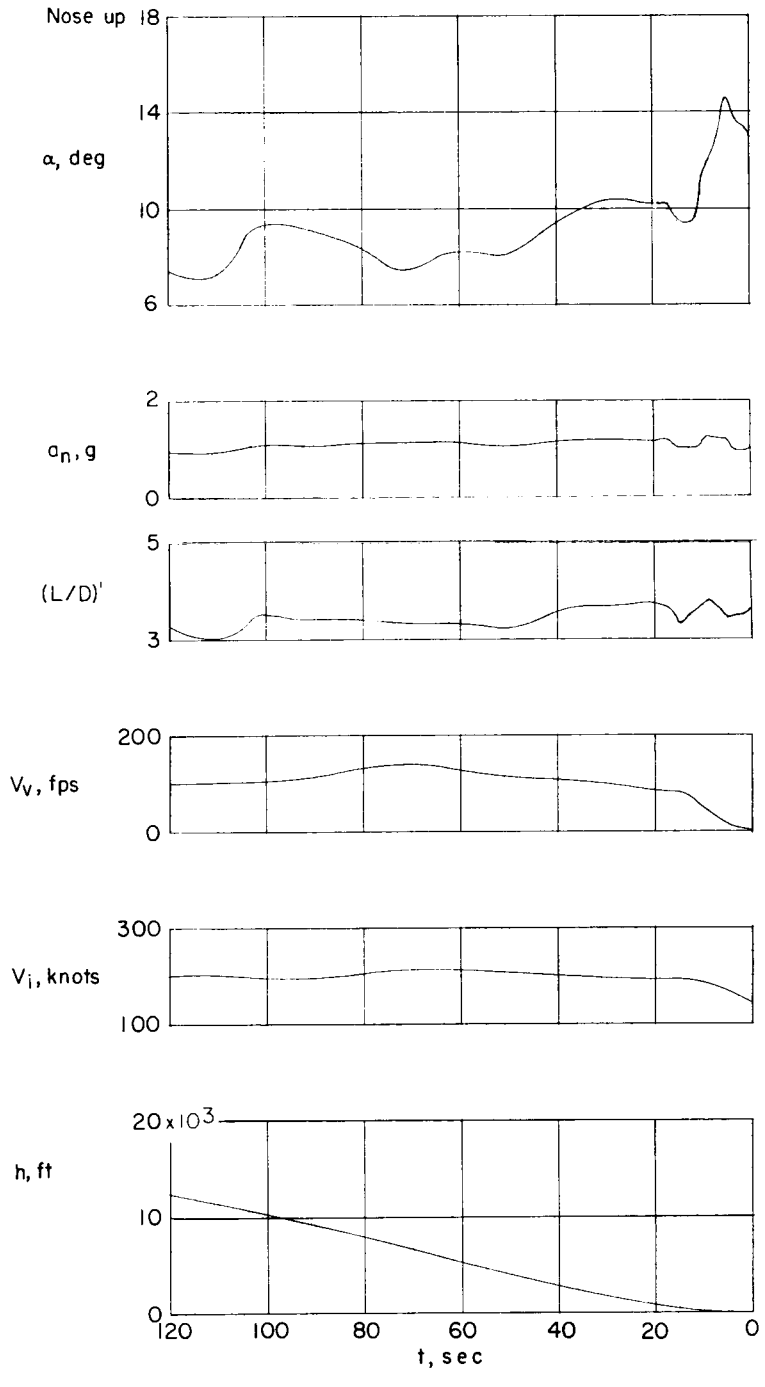

(b) Time history of the approach and landing.

Figure 4.- Continued.

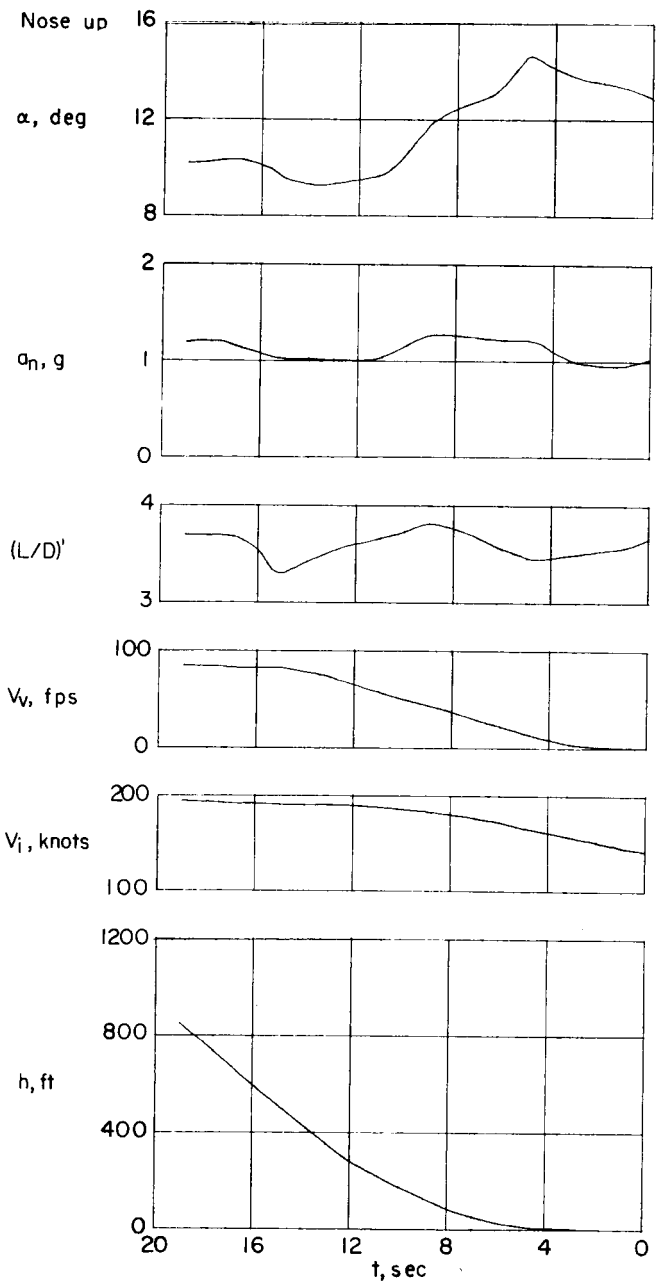

(c) Time history of the flare.

Figure 4.- Concluded.

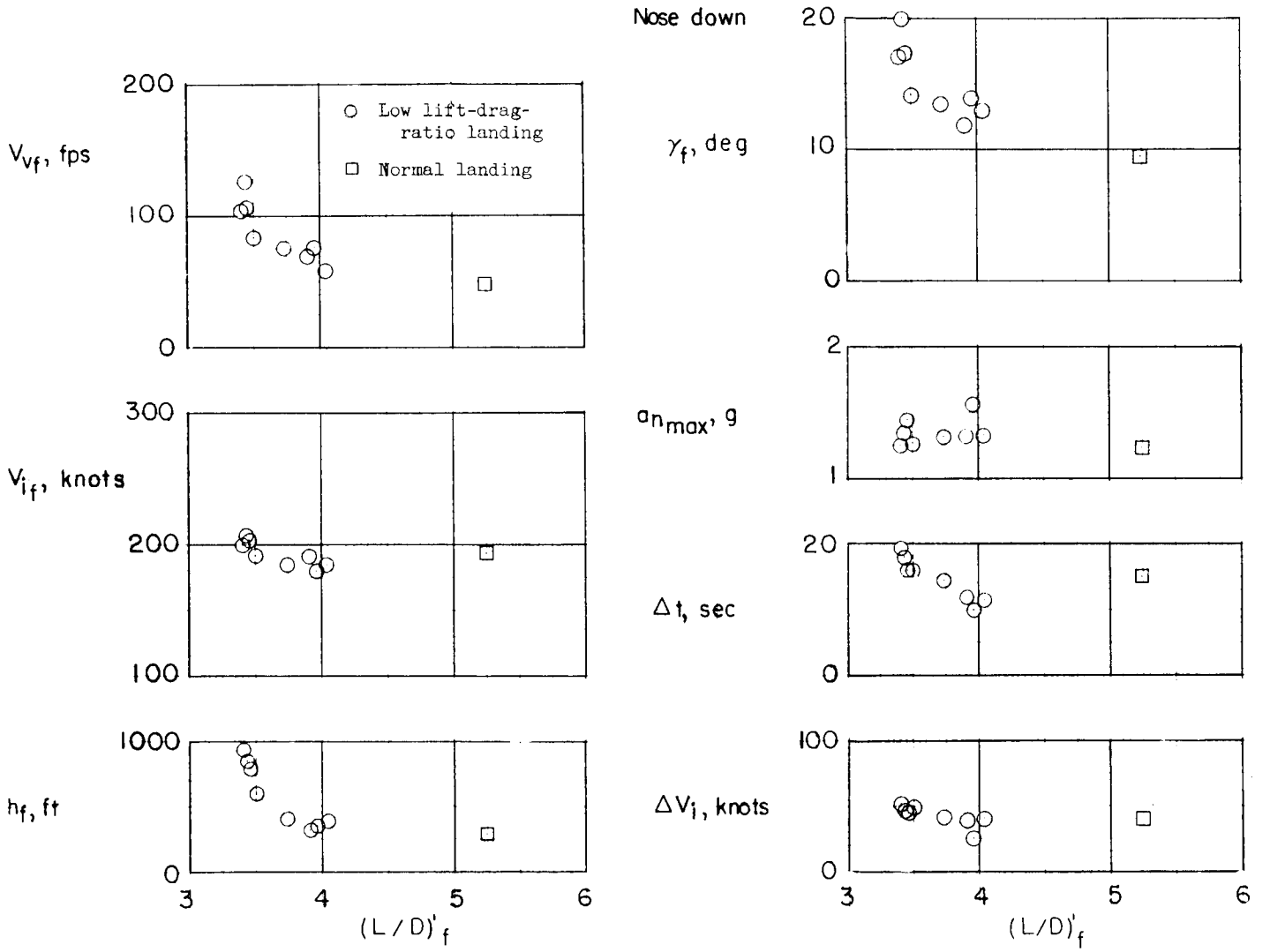

Figure 5.- Characteristics of final-flare parameters.

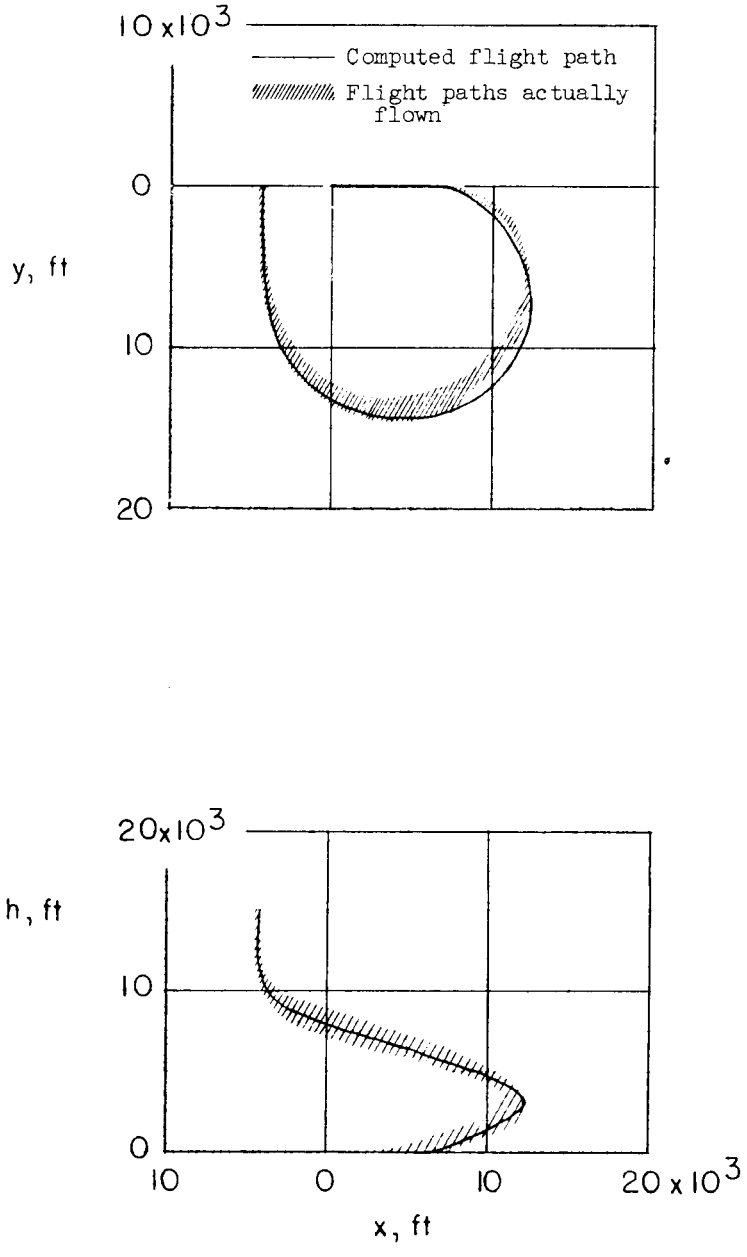

Figure 6.- Comparison of computed landing patterns with patterns actually flown. V_i = 200 KIAS; $\varphi = 30^\circ$.

NASA - Langley Field, Va. H-138